Alaa Alasadi (iD), F. Claeyssens, and D. A. Allwood

View Online   Export Citation   CrossMark

Laser direct writing (LDW) of magnetic structures

Alaa Alasadi,[1,2,a] F. Claeyssens,[1] and D. A. Allwood[1]
[1]*Department of Materials Science and Engineering, University of Sheffield, Sheffield, UK*
[2]*Karbala Technical Institute, Alfurat Alawsat Technical University, Iraq*

Laser direct writing (LDW) has been used to pattern 90nm thick permalloy ($Ni_{81}Fe_{19}$) into 1-D and 2-D microstructures with strong shape anisotropy. Sub-nanosecond laser pulses were focused with a 0.75 NA lens to a 1.85μm diameter spot, to achieve a fluence of approximately 350 mJ.cm^{-2} and ablate the permalloy film. Computer-controlled sample scanning then allowed structures to be defined. Scan speeds were controlled to give 30% overlap between successive laser pulses and reduce the extent of width modulation in the final structures. Continuous magnetic wires that adjoined the rest of the film were fabricated with widths from 650 nm - 6.75μm and magneto-optical measurements showed coercivity reducing across this width range from 47 Oe to 11 Oe. Attempts to fabricate wires narrower than 650nm resulted in discontinuities in the wires and a marked decrease in coercivity. This approach is extremely rapid and was carried out in air, at room temperature and with no chemical processing. The 6-kHz laser pulse repetition rate allowed wire arrays across an area of 4 mm x 0.18 mm to be patterned in 85 s. © *2018 Author(s). All article content, except where otherwise noted, is licensed under a Creative Commons Attribution (CC BY) license (http://creativecommons.org/licenses/by/4.0/).* https://doi.org/10.1063/1.5007227

INTRODUCTION

Patterned magnetic microstructures are used in many applications such as actuators,[1] sensors[2–4] and control of magnetic particles[5] or magnetically-labelled cells.[6] There are various approaches to fabricating nanoscale and microscale magnetic structures, including electron beam lithography,[7–9] photolithography,[7,10] X-ray lithography,[7,11] focused-ion-beam milling[12,13] and scanning probe lithography.[14] Each fabrication technique brings particular advantages and disadvantages in terms of resolution, flexibility, speed, complexity and cost.

Laser direct writing (LDW) is an alternative approach to creating planar structures and has been used to pattern many materials, including Cu,[15] Ag,[16,17] Al[18] and Au.[19] It offers a rapid and uncomplicated single-step direct write procedure that allows design flexibility in the fabrication of one-to three-dimensional structures with high resolution.[20] In general, LDW techniques fall into three main categories depending on whether material is removed (LDW-), modified (LDWm) or added (LDW+).[20,21] Laser ablation is used to perform LDW- techniques by removal of precise quantities of materials. The ablation process depends on the laser wavelength, intensity and pulse duration, in addition to the optical and thermal properties of materials.[22,23] Laser ablation with nanosecond pulse widths is initiated when a material absorbs sufficient energy from a laser pulse to reach its melting point, which occurs at a threshold laser fluence.[22–24]

In this paper, we report the use of LDW- to form microscale structures from thin films of the ferromagnetic alloy $Ni_{81}Fe_{19}$ (permalloy). We also present microscopy of the resulting structures and use magneto-optical measurements to demonstrate the structures' shape-dependent magnetic properties.

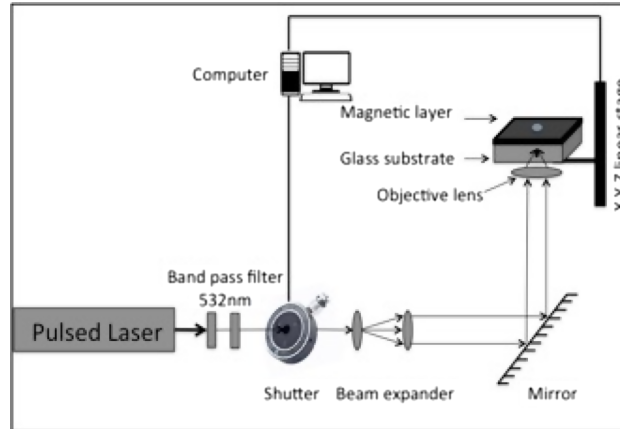[a]Electronic mail: alaaalasady74@yahoo.com

FIG. 1. Schematic of the laser ablation system with main three parts of LDW: laser source, laser beam delivery system and sample/platform scanning system.

EXPERIMENTAL

Permalloy thin films of 90 nm thickness were deposited on glass substrates by thermal evaporation at a rate of 0.4 Å.s^{-1} in a system with a base pressure of 10^{-7} mbar.

Figure 1 shows the experimental arrangement for the LDW-system. An Alphalas passively Q-switched diode-pumped solid-state semiconductor laser was used at a pulse repetition rate of 6kHz. A bandpass filter (532 ± 2 nm) was used to select the frequency doubled 532 nm wavelength only. The resulting pulse width was 800 ps and the beam profile showed the TEM$_{00}$ mode. Maximum pulse energy at maximum repetition 40 kHz rate is 4.6 μJ. Pulse energy was attenuated using absorptive neutral density filters to 10 nJ. An external laser shutter (UNIBLITZ LS6ZM2-nl) was used to control the exposure time. The laser beam was directed to a 0.75 NA objective lens to focus the laser beam onto the sample. The laser ablation spot diameter was 1.85 μm. A three-axis (x, y, z) system of motorized linear stages (Aerotech ANT130-XY and PRO115 for Z-direction) allowed the sample to be scanned under computer control to 5nm precision and at speeds of up to 2 m/s.

The number of pulses per length unit, N was controlled by setting the scan speed, v, of the sample and is given by:
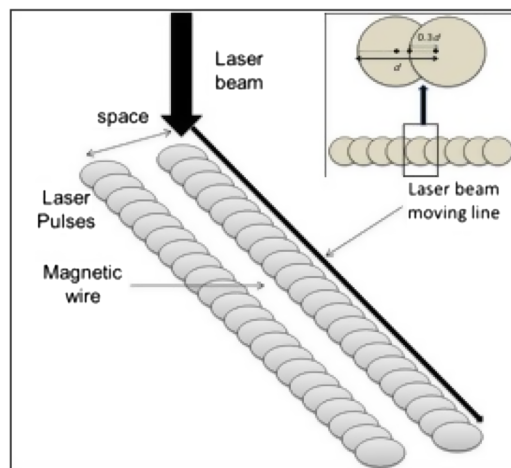
$$N = \frac{f}{v} \tag{1}$$

FIG. 2. Diagram showing overlap of successive laser pulses, and the formation of wires by laser ablation removal of unwanted areas of a film to form a wire between two ablation lines.

The magnetic structures were patterned in single steps by removing unwanted areas of material from the substrates with 30% overlap between laser pulses. This means that the edge profile of any magnetic wire fabricated in this way will not be straight but will show the undulation caused by the change in laser position between pulses (Fig. 2). The dimensions and edge profile of the wire is therefore controlled by the pulse diameter, overlap and separation of adjacent ablation line scans.

The overlap, D, between successive laser pulses was calculated by:

$$D = \frac{-(N \cdot d) + 1}{N} \tag{2}$$

where d is a laser spot diameter, so that $D > 0$ for separated laser spots, $D = 0$ for ablation spots just touching and $D < 0$ for overlapping ablation regions.

The magnetic properties of structures were measured using a custom built focussed magneto-optic Kerr effect (MOKE) system similar to the system described elsewhere.[25] Samples were measured in the longitudinal MOKE configuration under an alternating current (ac) applied magnetic field at a frequency of approximately 27 Hz using a continuous wave (CW) laser of wavelength 532 nm (Coherent Verdi V2). The MOKE instrument was operated with a focal spot of approximately 4 μm × 7 μm (full-width-at-half-maximum) on the sample and used high quality Glan-Taylor polarisers. Atomic force microscopy (AFM; Veeco, Dimension^{TM} 3100) and scanning electron microscopy (SEM; Raith EO FE-SEM) were used to image the magnetic structures.

RESULTS AND DISCUSSION

Magnetic wires of different widths were fabricated by varying the spacing between ablation lines between 2 μm and 8.6 μm. These were fabricated using a laser fluence just above the 350 mJ.cm^{-2} ablation threshold for our film. Figure 3 shows examples of such structures for ablation line separations of 2.5 μm – 8.6 μm to give magnetic wires of widest width 650 nm – 6.75 μm. The wider wires are relatively well defined and have a periodic edge structure that reflects the separation of adjacent laser pulses during the ablation process. This edge structure has measured amplitude of 125 nm for all wire widths and results in narrower wires beginning to lose definition.

Figure 4 shows images of wires created with even narrower ablation line spacing (2.4 μm–2.0 μm). These are less well defined still with significant amounts of non-ablated material. However, the wire
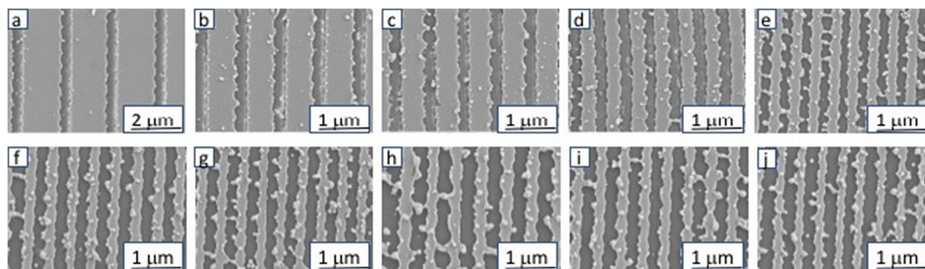

FIG. 3. Scanning electron micrographs of permalloy wires created with laser ablation line separations of a) 6.75 μm, b) 3.75 μm, c) 2.75 μm, d) 1.75 μm, e) 1.25 μm, f) 1.15 μm, g) 950 nm, h) 850 nm, i) 750 nm and j) 650 nm. The light regions are the magnetic material while the dark regions are ablated areas.

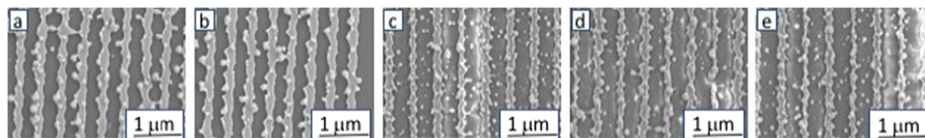

FIG. 4. Scanning electron micrographs of wires created with laser ablation line separations of a) 550 nm, b) 450 nm, c) 350 nm, d) 250 nm and e) 150 nm with different spaces between magnetic wires. The light regions are the magnetic wires while the dark are ablated areas.
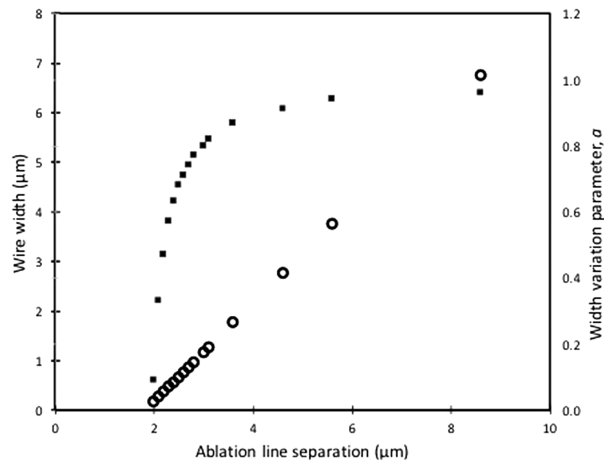
FIG. 5. The ablation line separation as function to; wire widths and width variation parameter (*a*). Structural parameters of LDW- fabricated wires with 1.85 μm diameter laser spot and 30% spot overlap. Wire width shown is the average of minimum and maximum wire widths, while *a* is the ratio of the minimum to maximum wire widths.

structures remain evident and we could obtain structures with width as narrow as 150 nm (2 μm ablation line spacing; Fig. 4e).

We can characterise the edge structure of the wires as a width variation parameter, *a*, defined as the ratio of the minimum and maximum wire widths measured across multiple positions, so that *a* = 1 for parallel edges and *a* < 1 for wave-like edges. The structural parameters of these wires are represented as in figure 5, with wire widths shown as an average of the minimum and maximum measured widths for each wire type. The reduced width of wires formed using more closely spaced ablation lines necessarily creates a larger relative width variation and, therefore, reduced values of *a*. Wires with reduced width variations (higher *a*) can be obtained with increased laser spot overlap (*D*). AFM analysis (Fig. 6) appears to show that the ablation process appears to result in redeposition of material at the edges of structures, where the laser power is close to the ablation threshold.

This fabrication process is extremely rapid. For example, at the scan speed used of 7.5 mm.s^{-1}, the time required to fabricate 75 magnetic wires each of dimensions 550 nm × 4.0 mm is, in principle, 40s. In practice, this increased to 85 s due to the time required to change the scan direction at the end of each line. This gives an effective fabrication rate of 3.5 mm.s^{-1}, although this will vary with the design of structures and with the scanner or translation stages employed. Higher repetition rate, scan speed and, for larger structures, larger focal spot size will also have a marked impact on the fabrication speed.

Figure 7 shows MOKE hysteresis loops obtained from the wire arrays for wire widths down to 650 nm (Fig. 7a–j). These were obtained with the Kerr sensitivity direction and applied field along
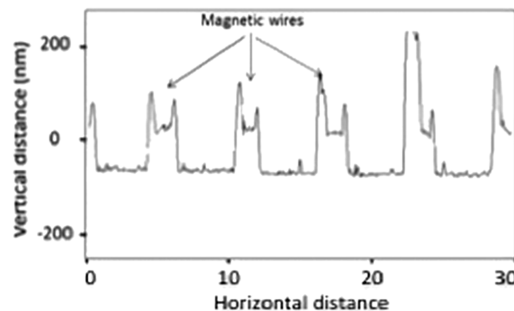

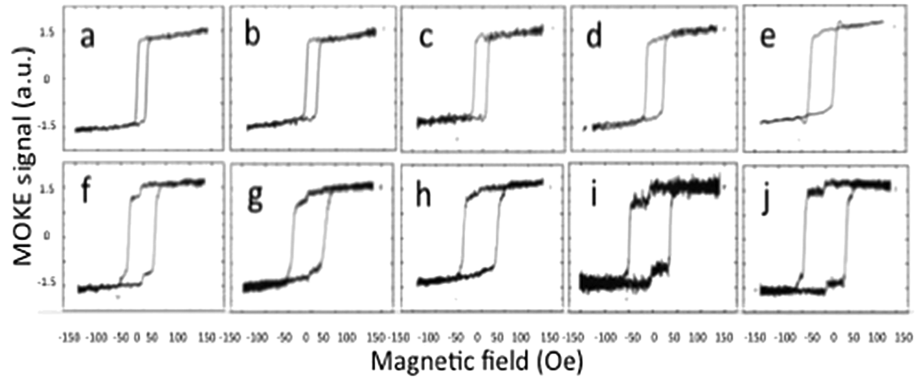FIG. 6. Atomic force microscopy section analysis of 1.75 μm wide permalloy wire fabricated by LDW.

FIG. 7. MOKE hysteresis loops of LDW-fabricated permalloy wires of width (a) 6.75 µm, (b) 3.75 µm, (c) 2.75 µm, (d) 1.75 µm, (e) 1.25 µm, (f) 1.15 µm, (g) 950 nm, (h) 850 nm, (i) 750 nm and (j) 650 nm.

the wires' long axis. All loops have notable easy axis character with sharp magnetization reversal transitions, which indicates that the LDW-fabricated structures exhibit strong shape anisotropy and may reverse via rapid propagation of domain walls injected from the adjoining film. The low-field steps observed in the narrowest wires (Fig. 7i and j) are due to detection of Kerr signal from the surrounding film, which contributes a relatively large signal compared to that of the small structures. Figure 8 shows MOKE loops obtained from even narrower wires, down to 150 nm in width. Despite the apparently poor physical appearance of these structures (Fig. 4) the magnetization reversal transitions in hysteresis loops remain reasonably sharp until the very narrowest case (Fig. 8e).
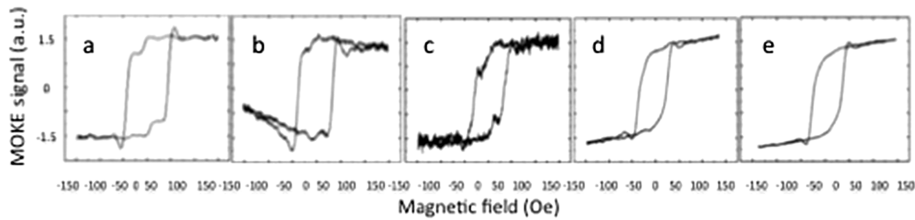

FIG. 8. MOKE hysteresis loops of LDW-fabricated permalloy wires of width (a) 550 nm, (b) 450 nm, (c) 350 nm, (d) 250 nm and (e) 150 nm.
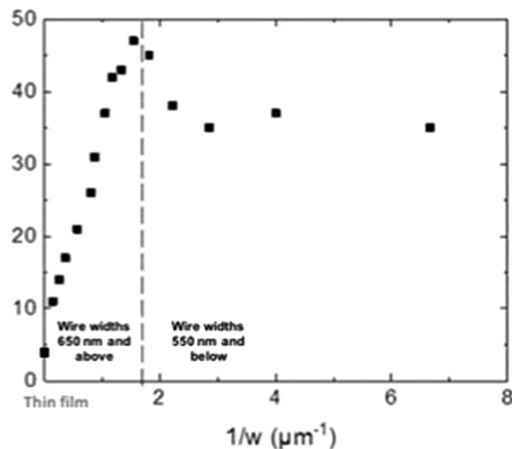

FIG. 9. Magnetic coercivity as function of inverse wire widths.

The coercivity of the wires (Fig. 9) is proportional to the inverse of wire width for structures at least 650 nm wide. This is commonly observed for well-defined soft ferromagnetic wire structures[26] but is perhaps surprising to see here given the edge profile of the laser-patterned wires. However, coercivity falls with wire width below 650 nm as the definition of the wire edges becomes increasingly poor and, in all likelihood, domain wall pinning becomes stronger.

CONCLUSIONS

In this work, we have demonstrated pulsed laser direct writing (LDW-) ablation can be used to fabricate microscale structures from a 90 nm thick permalloy thin film. The sample scan speed and laser pulse rates gave a 30% overlap between neighbouring focused laser spots. This produced a periodic profile to the edges of fabricated wires that became relatively more pronounced for narrower wires. Wires from several micrometres to 150 nm in width could be fabricated although wire widths less than 650 nm had significant levels of additional material. Similarly, wider wires (650 nm or more) exhibited clear uniaxial behaviour and coercivity proportional to the inverse of wire width.

LDW offers many benefits in the fabrication of nano-microscale structures. This process is a simple, low cost one-step processing without the use of corrosive chemicals, which enables flexibility in sample design and high throughput. The fabrication rate here of 3.5 mm.s^{-1} can be increased further with different system design. This makes LDW particularly suitable for fabrication of low numbers of elements or for prototyping.

ACKNOWLEDGMENTS

[1] A. Arani, A. Eskandari, P. Ouyang, and R. Chopra, Smart Mater. Struct. **26**, 87001 (2017).

[2] D. K. Wood, K. K. Ni, D. R. Schmidt, and A. N. Cleland, Sensors Actuators A Phys. **120**, 1 (2005).

[3] M. Vázquez and A. Hernando, J. Phys. D. Appl. Phys. **29**, 939 (1996).

[4] A. Sobczak-Kupiec *et al.*, Nanomedicine Nanotechnology, Biol. Med. **12**, 2459 (2016).

[5] Q. A. Pankhurst, N. T. K. Thanh, S. K. Jones, and J. Dobson, J. Phys. D. Appl. Phys. **42**, 224001 (2009).

[6] J. Pintaske, B. Müller-Bierl, and F. Schick, Phys. Med. Biol. **51**, 4707 (2006).

[7] J. I. Martín, J. Nogués, K. Liu, J. L. Vicent, and I. K. Schuller, J. Magn. Magn. Mater. **256**, 449 (2003).

[8] P. B. Fischer and S. Y. Chou, Appl. Phys. Lett. **62**, 6 (1993).

[9] J. Anne Currivan, J. Vac. Sci. Technol. B, Nanotechnol. Microelectron. Mater. Process. Meas. Phenom. **32**, 021601 (2016).

[10] T. Huong Au, D. Thien Trinh, D. Bich Do, D. Phu Nguyen, Q. Cong Tong, and N. Diep Lai, Phys. B Condens. Matter (2017).

[11] F. Rousseaux *et al.*, J. Vac. Sci. Technol. B Microelectron. Nanom. Struct. Process. Meas. Phenom. **13**, 2787 (1995).

[12] G. Xiong, D. A. Allwood, M. D. Cooke, and R. P. Cowburn, Appl. Phys. Lett. **79**, 3461 (2001).

[13] J. Lohau, A. Moser, C. T. Rettner, M. E. Best, and B. D. Terris, Appl. Phys. Lett. **78**, 990 (2001).

[14] E. Albisetti *et al.*, Nat. Nano **11**, 545 (2016).

[15] K. Kordás, K. Bali, S. Leppävuori, A. Uusimäki, and L. Nánai, Appl. Surf. Sci. **154**, 399 (2000).

[16] T. Baldacchini *et al.*, Opt. Express **13**, 1275 (2005).

[17] Z. Zhao, G. He, M. Zheng, X. Dong, J. Liu, and F. Jin, Appl. Phys. Lett. **110**, 263113 (2017).

[18] T. Cacouris, G. Scelsi, P. Shaw, R. Scarmozzino, R. M. Osgood, and R. R. Krchnavek, Appl. Phys. Lett. **52**, 1865 (1988).

[19] R. L. Harzic, J. Laser Micro/Nanoengineering **3**, 106 (2008).

[20] C. B. Arnold and A. Piqué, MRS Bull. **32**, 9 (2007).

[21] A. Lisiecki, J. Kusinski, S. Kac, A. Kopia, A. Radziszewska, M. Rozmus-Górnikowska, B. Major, L. Major, and J. Marczak, Bulletin of the Polish Academy of Sciences: Technical Sciences **60**, 711 (2012).

[22] G. Paltauf and P. E. Dyer, Chem. Rev. **103**, 487 (2003).

[23] K. Sokolowski-Tinten and D. von der Linde, Appl. Surf. Sci. **154**, 1 (2000).

[24] K. H. Leitz, B. Redlingshöer, Y. Reg, A. Otto, and M. Schmidt, Physics Procedia **12**, 230 (2011).

[25] R. P. Cowburn, D. A. Allwood, M. D. Cooke, and G. Xiong, J. Appl. Phys. **36**, 2175 (2003).

[26] K. J. Kirk, J. N. Chapman, S. McVitie, P. R. Aitchison, and C. D. W. Wilkinson, Appl. Phys. Lett. **75**, 3683 (1999).